SRS Station MPW6.2 - A New Facility for variable energy SAXS/WAXS at the Daresbury Laboratory

N. J. Terrill[1], G. Bushnell-Wye[1], R. J. Cernik[1,2,3], A. J. Dent[1], G. P. Diakun[1], C. J. V. Flaherty[1], J. Kay[1], C. Tang[1], P. Barnes[2], G. N. Greaves[4], T. Rayment[5] and A. Ryan[6]

[1] Daresbury Laboratory, Warrington WA4 4AD, UK
[2] Department of Crystallography, Birkbeck College, London WC1E 7HX
[3] Manchester Materials Science Centre, University of Manchester and UMIST, Grosvenor St, Manchester M1 7HS
[4] Department of Physics, The University of Wales, Aberystwyth, Penglais, Aberystwyth, Ceredigion, SY23 3BZ
[5] Department of Chemistry, University of Cambridge, Cambridge CB2 1TN, UK
[6] Department of Chemistry, University of Sheffield, Western Bank, Sheffield S10 2TN, UK

Fibre Diffraction Review **11**, 20-27, 2003

ABSTRACT

Station 6.2 has entered its commissioning phase having taken "first light" in November 2001 (Fig. 1). A team comprising elements from SRD, ID and ED departments at Daresbury Laboratory (Fig. 2) built the beamline. The project has also benefited from the scientific direction given by four University Partners: Dr. Trevor Rayment - Department of Chemistry, University of Cambridge; Prof. Neville Greaves - Department of Physics, University of Aberystwyth; Prof. Tony Ryan - Department of Chemistry, University of Sheffield and Prof. Paul Barnes - Department of Crystallography, Birkbeck College London. The project, funded by the EPSRC, forms part of the SRS upgrade which began in 1998. The commissioning phase is due to be completed in December 2002 and the Station should be handed over for user operations in the spring of 2003.

Introduction

Significant advances in technology over recent years have resulted in scientists who use the SRS requiring sample cells that mimic the real world ever more closely. As a result they require facilities that can collect data faster and on smaller or more dilute systems. Pressure, temperature, pH, humidity and the presence of corrosive atmospheres are all part of the current experimental trend. The new beamline is capable of taking full advantage of the high flux generated by MPW 6 to deliver high quality research in all of the above areas with unprecedented accuracy and at millisecond timescales.

X-ray delivery and Optics

A ten-pole wiggler, identical in design to that installed on beamline 14 and described by Duke *et al.* (1998) has been installed in straight section 6 (Fig. 3) of the SRS. The characteristics for the source can be found in Appendix A.

The X-ray flux output of the device reaches a peak at approximately 8 keV. The practical photon energy

Figure 1: First light in the MPW 6.2 Experimental Hutch.

range (5 to 18 keV) is defined by beryllium window absorption at low energy and the high-energy flux limit from the 2T magnetic poles of the insertion device. The total radiation fan from the multipole wiggler on beamline 6 has been split into two sections 9.8 m from the tangent point. A plane mirror deflects 7.5 mrad of beam in the UV energy range for use in station MPW6.1 (Bowler *et al.*, 2002). The first beamline element on MPW6.2 is a water-cooled defining aperture at 12.88m that defines an X-ray beam of 4.5 mrad (horizontal) and 1.4 mrad (vertical). This is followed by a set of

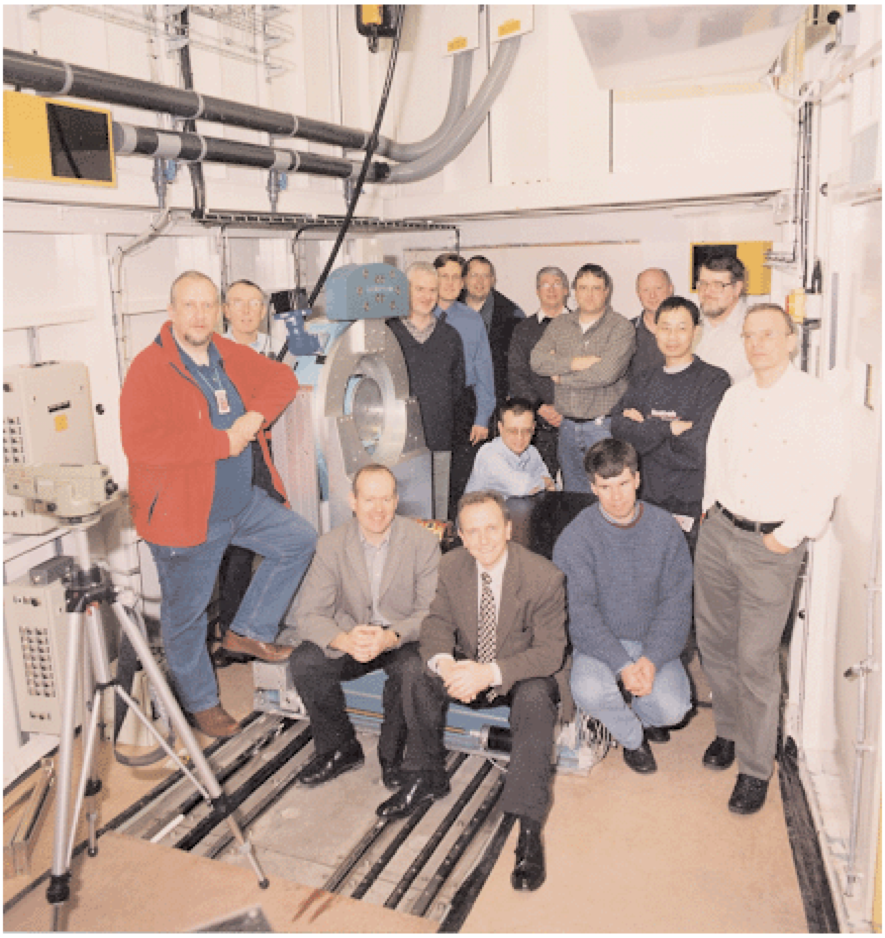

Figure 2: The DL team responsible for the project.

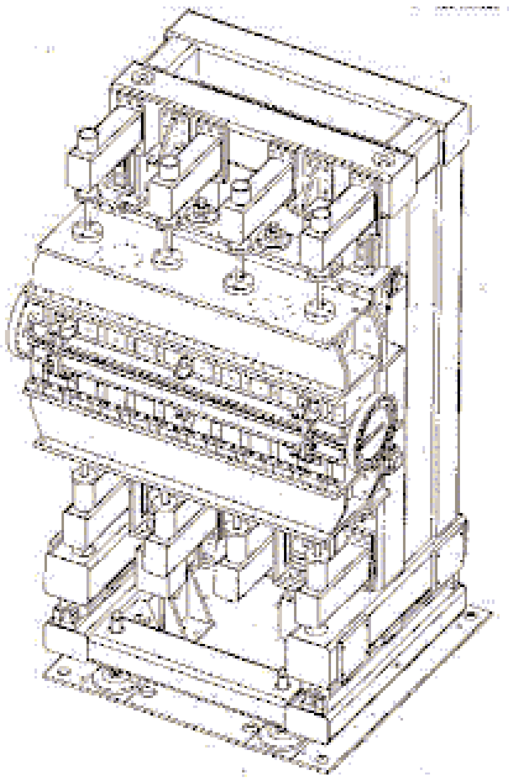

Figure 3: A schematic of the MPW insertion device from which Station 6.2 will obtain its X-rays.

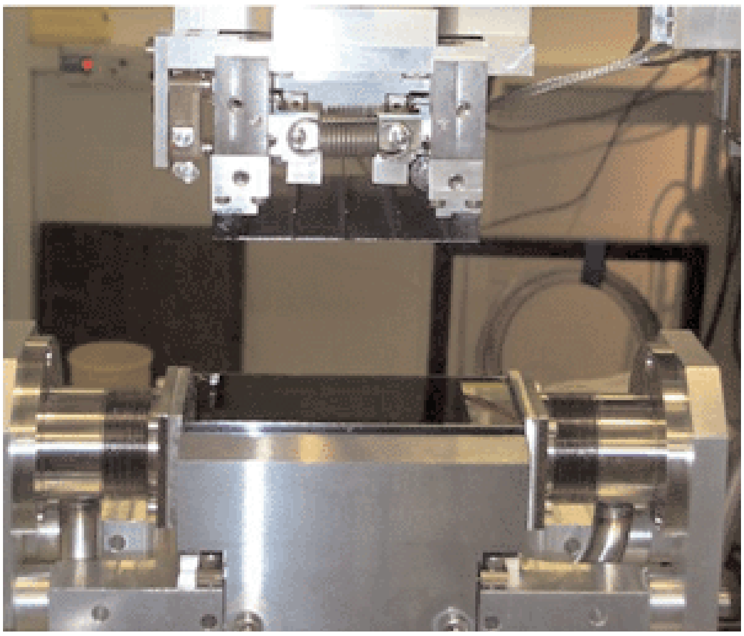

Figure 4: Sagittal Monochromator showing ribs of top crystal.

water-cooled slits. The beam is then collimated by the first of two identical planar, cylindrically bent, Si mirrors (1200 x 120 x 50 mm with a 500 Å rhodium coating). The sagittal-crystal monochromator, designed by Bilsborrow *et al.* (in preparation) and shown in Figure 4, gives both energy selection and horizontal focussing. The monochromator has a flat, water-cooled, first crystal cut along the [111] direction. The second Si crystal, also cut along the [111] direction, is sagittally bent and collects the entire available horizontal aperture. It has 4 ribs to prevent anticlastic bending. The focal point of the second crystal can be adjusted to any point in the experimental area over a range of 5 m.

A second set of slits, immediately after the monochromator, provides further beam definition. These slits directly precede a second mirror, which provides vertical focussing for the beamline. A third set of slits has been installed after the mirror and is in turn followed by the station stop. The monochromator and mirror systems are all contained within a separate optics hutch in order to reduce parasitic scattering. Two further sets of slits are accommodated in the experimental hutch to reduce parasitic scatter still further for SAXS experiments. The overall beamline layout is shown in Figure 5.

Experimental Station

The experimental station is designed on a modular basis for complete flexibility. Unlike other NCD stations at the SRS, the station does not have an optical bench so experiments can be built up from the floor of the hutch giving extra versatility in sample environment design. A system of rails has been incorporated into the floor of the hutch to aid alignment. The two options in Figure 6 are representative of what is possible, but are by no means exhaustive. SAXS cameras can be built to any length between 1m and 4m with 25cm intervals. Coupled to the energy capabilities, this leads to a very adaptable station environment indeed.

Detectors

The beamline has been built to take advantage of recent developments in detector technology. The centrepiece of the new station, and its most significant development, is the SAXS/WAXS gas multiwire detector combination based on RAPID technology (Helsby *et al.*, 2002). The SAXS detector system, whose funds were included in the project costs, has a 60° quadrant with radius 200mm. The detector is capable of global count rates in excess of 10MHz, with peak resolutions (FWHM) of about 400 µm using 1024 pixels. The curved position sensitive detector for measuring WAXS spectra, also funded by the EPSRC in a separate grant, has a complex and rapid way of interpolating the diffraction peaks (Fig. 7). This enables the detector to obtain a peak resolution of better than 0.06° and data to be collected in milliseconds. This timescale and statistical precision will be a much better match for the complementary small-angle scattering and spectroscopy techniques also available on the station. The detector is capable of collecting 60° in 2θ at a global count rate of at least 10MHz.

Early Commissioning Tests

Initial tests of the station/detector combination have been promising. To give some idea of the quality of data from the WAXS detector, Figure 8 shows a comparison of data collected on HDPE with the INEL detector from Station 8.2. Data are clearly visible at 100µs using the new detector system whereas with the INEL information is difficult to resolve below 1s. A collagen standard sample collected in 120sec is shown to illustrate the quality of data available from the quadrant detector and to give some idea of **q**-range at 10keV with a 3m camera (Fig. 9). Commissioning is still ongoing with both detectors to establish a better understanding of end effects and energy response.

Table A - An illustration of the working range of the station.

Camera Length		MIN = 1000 mm				MAX = 4000 mm			
Limits of useful detector / mm		min = 8.27		max = 195.23		min = 8.27		max = 195.23	
Energy / keV	Wavelength / Å	d_{max} / Å	±	d_{min} / Å	±	d_{max} / Å	±	d_{min} / Å	±
5	2.48	300	14	12.88	0.02	1200	56	51	0.10
8	1.55	188	9	8.05	0.02	750	35	32	0.06
10	1.24	150	7	6.44	0.01	600	28	25	0.05
12	1.03	125	6	5.37	0.01	500	23	21	0.04
15	0.83	100	5	4.29	0.01	400	19	17	0.03
18	0.69	83	4	3.58	0.01	333	15	14	0.03

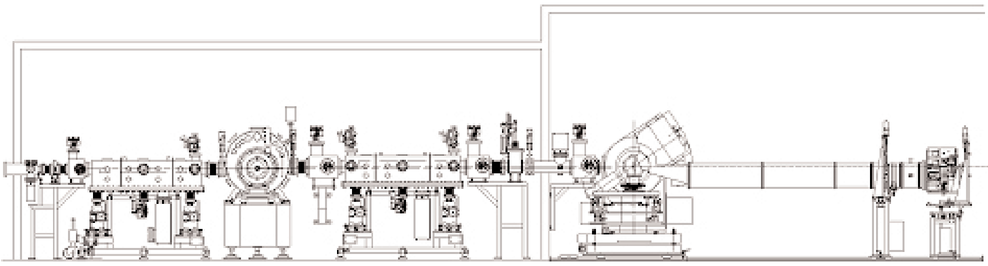

Figure 5: Beamline layout showing optics and experimental hutches.

a)

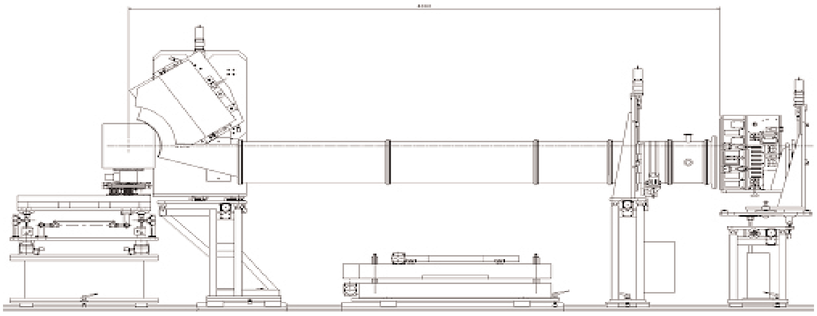

b)

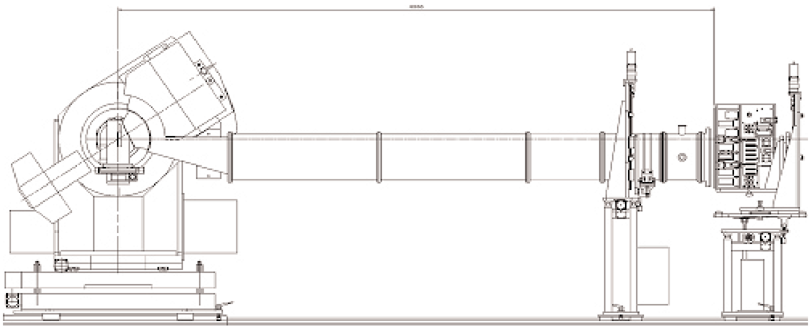

Figure 6: Station configuration options a) with 7-axis sample table and b) with 2-circle diffractometer with 3 axis sample mount.

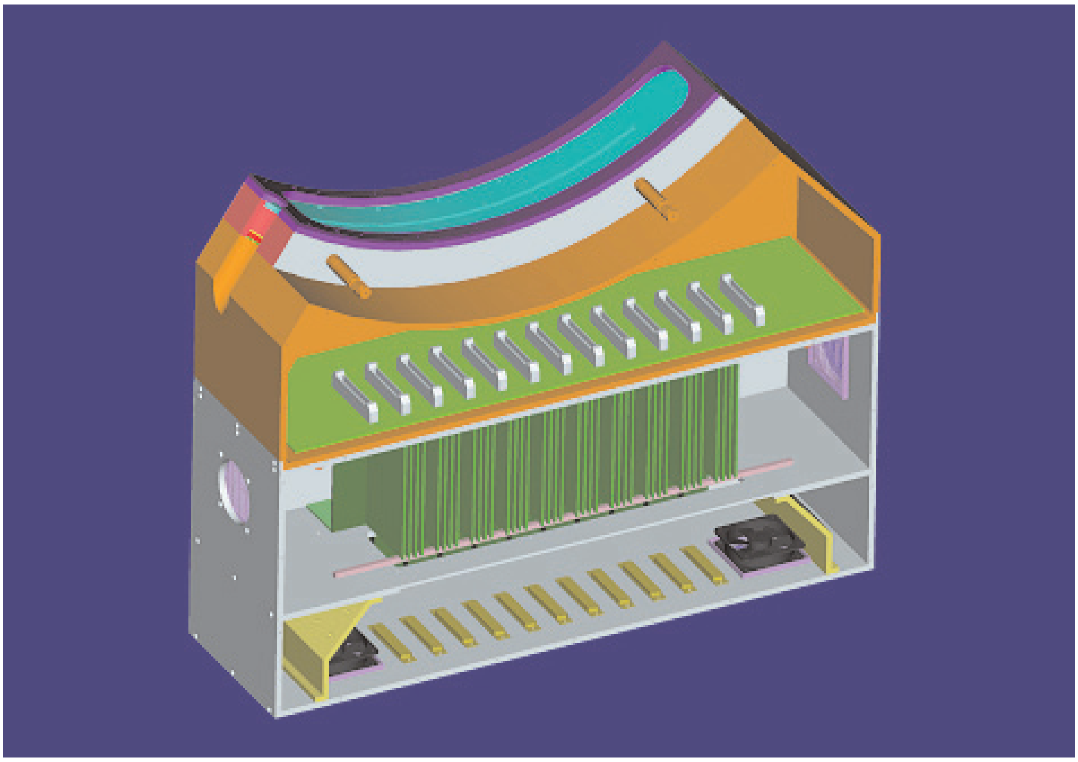

Figure 7: Schematic of the RAPID II Detector body showing basic arrangement of electrical components and connections.

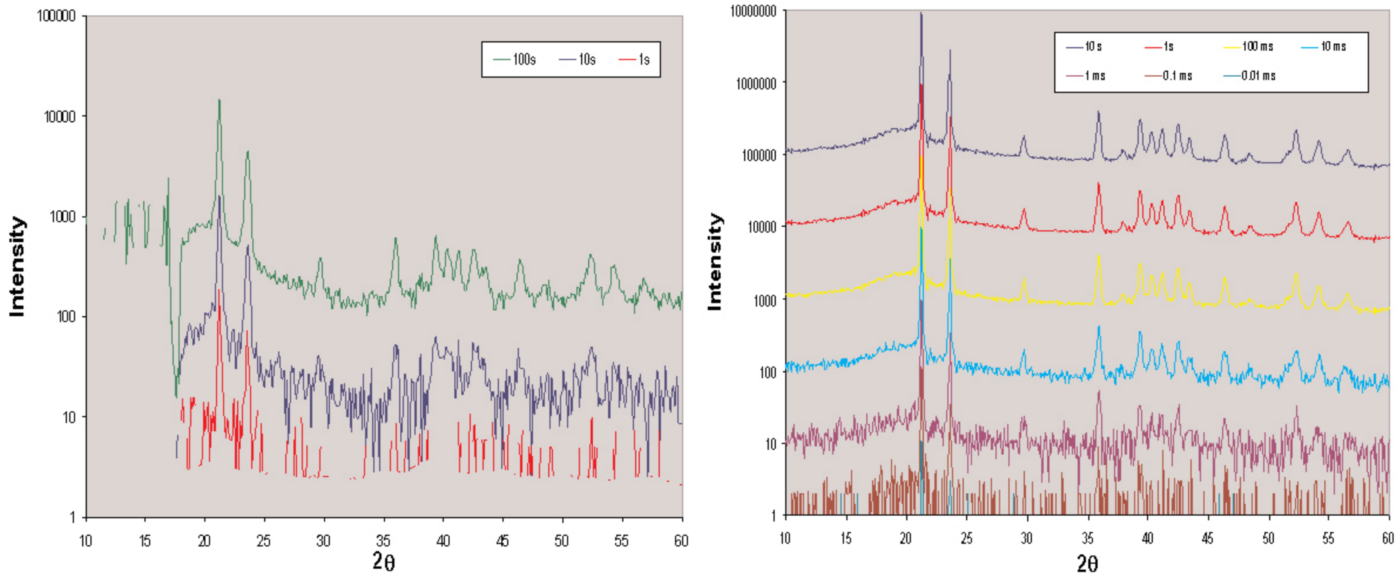

Figure 8: Spectra of the same HDPE sample collected by the INEL detector (left) and RAPID II (right).

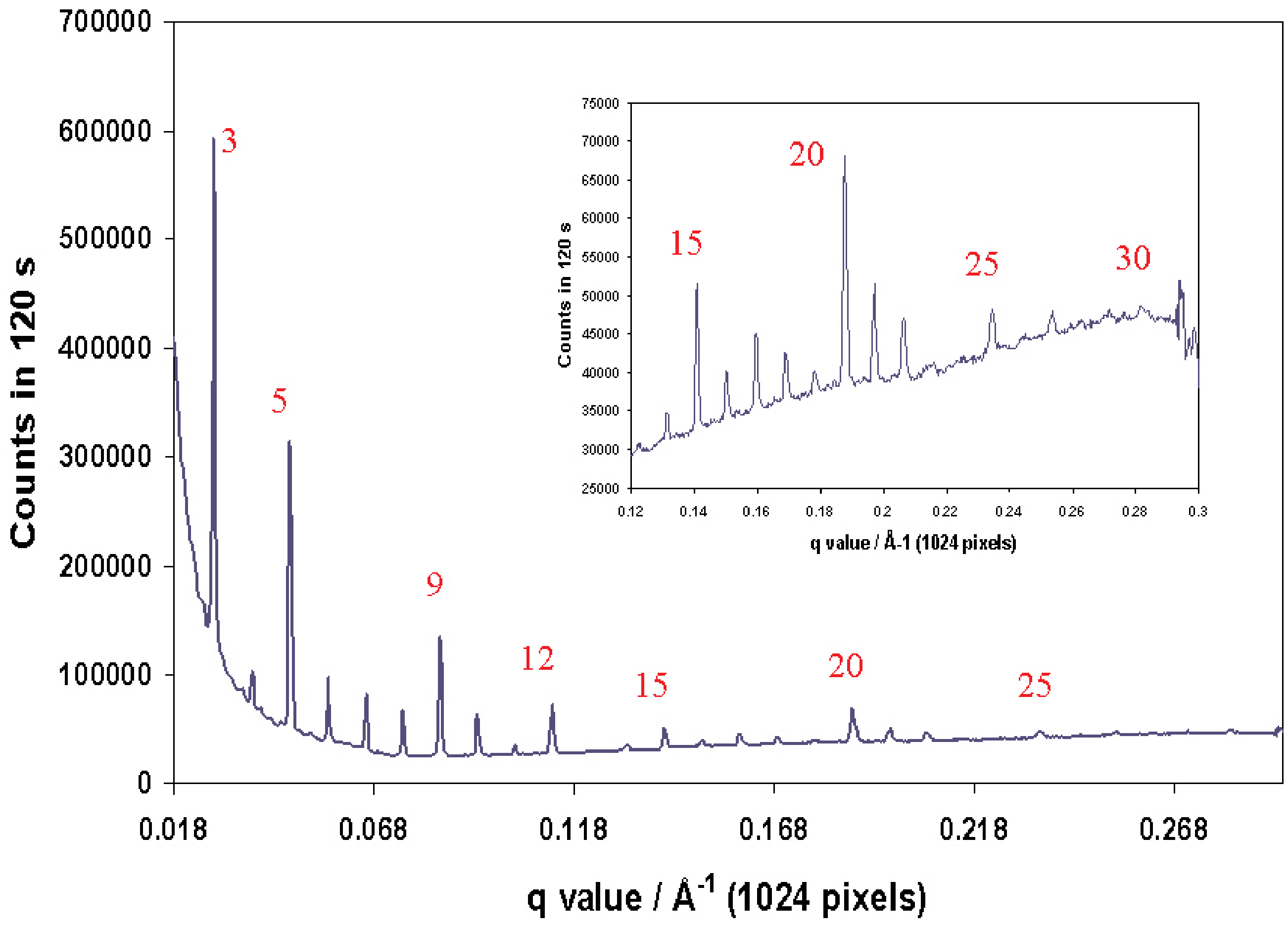

Figure 9: Collagen pattern collected at 3m and 10keV

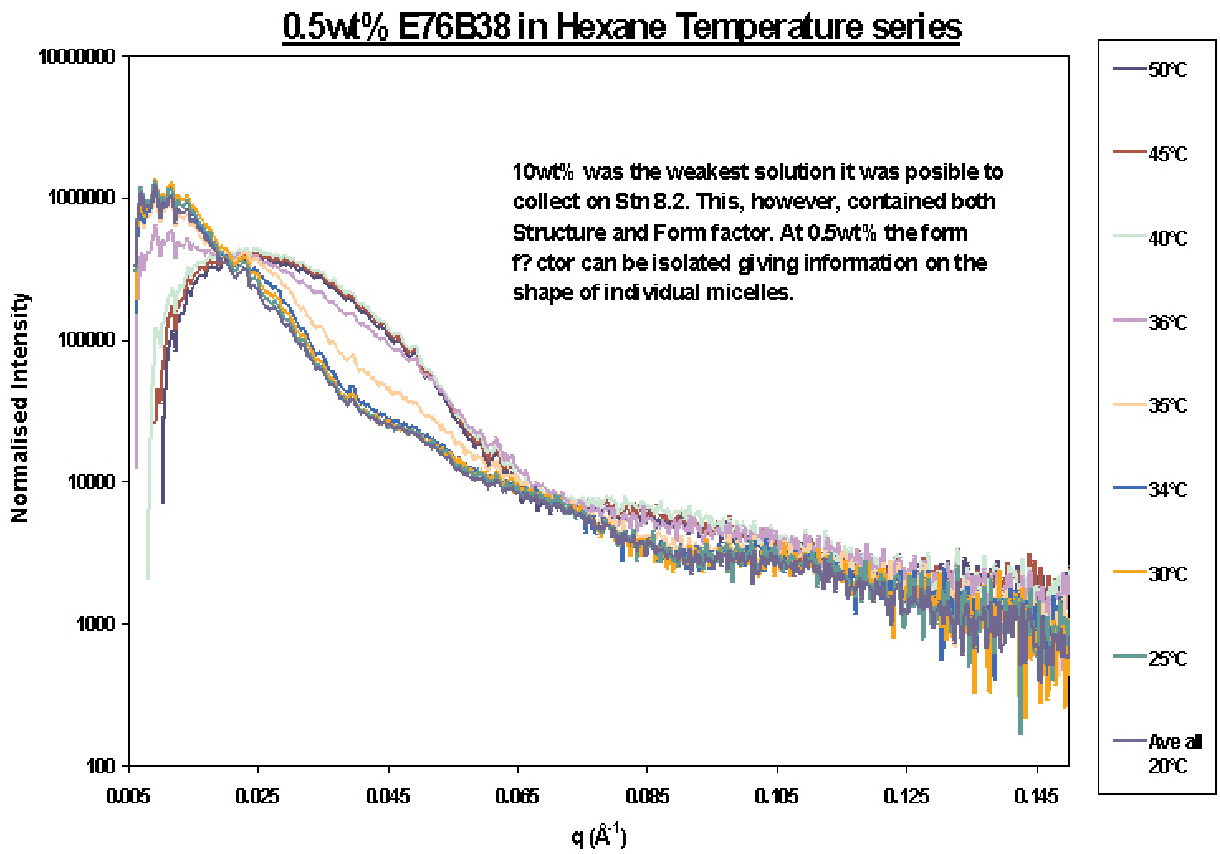

(a)

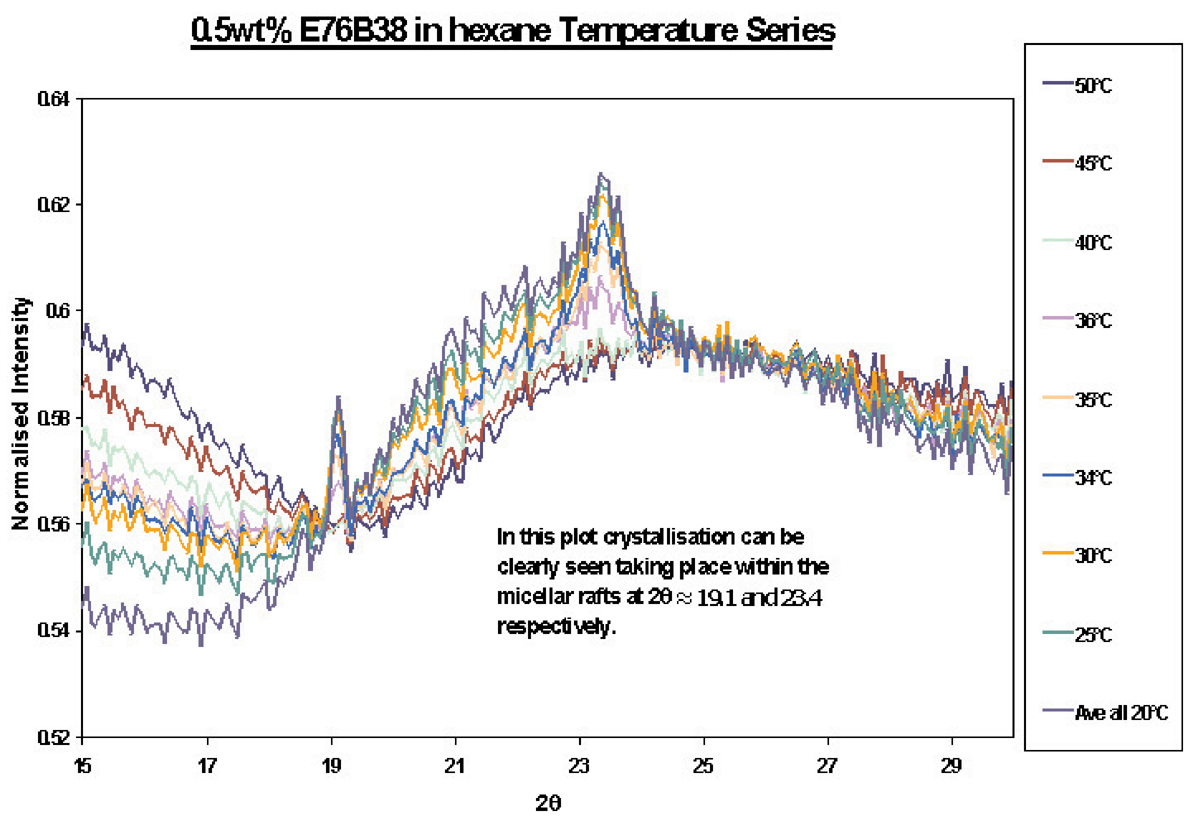

(b)

Figure 10 (a) and (b): Data taken with SAXS and RAPID II

Tests of the SAXS/WAXS combination were carried out by analysing a 0.5 wt% high-density polymer (E76B38) in hexane. Scientifically, this experiment was designed to examine crystallisation in constrained geometries. The block copolymer chains have two hydrophobic amorphous ends and a crystallisable centre. When the ethylene oxide crystallises, the micelle ends up with exposed hydrophilic sides. In a previous study on station 8.2, data from a 10 wt% solution were collected. However, the data contained both structure and form factor information. On station MPW 6.2 using the 0.5 wt% solution, the form factor could be isolated giving information on the shape of individual micelles (Fig. 10(a)). The corresponding wide-angle scattering data are shown in Figure 10(b), crystallisation can be clearly seen taking place within the micellar rafts at 2θ ≈ 19.1 and 23.4° respectively. Crystallisation at these low concentrations has not previously been observed.

The RAPID 2 wide-angle detector shows at least 3 orders of magnitude improvement over the INEL PSD previously used to collect diffraction data. However, the comparison with the INEL detector is perhaps less relevant, since there are much better detector systems available to users today. For example, the Dutch-Belgian beamline DUBBLE at ESRF (Borsbroom *et al.*, 1998) has an excellent user facility for SAXS/WAXS. The wide-angle component is based on gas-glass microstrip technology. This has inherently higher count rates than RAPID 2, but at present poorer angular resolution. Data collected recently by Ellen Heeley (Manchester Univ.) and Tony Ryan (Sheffield Univ.) demonstrate this point. Figure 11 shows the same polymer data set (Daplen iPP) collected (a) on DUBBLE and (b) on RAPID2 in approximately one hour. The rather poor appearance of the background in (b) is due to incomplete determination of the RAPID 2 instrumental resolution function. However, the count rate, peak height statistics and angular resolution are superior to the ESRF bending magnet beamline.

Future Developments

Closely associated with the project is the development of new data acquisition software. This forms part of the generic data acquisition project at the Daresbury Laboratory. A modular design has been adopted using a JAVA interface and a point and click approach to motor control. Data acquisition is also modular. It will be capable of taking sample environment modules written in a number of common equipment controls languages. Scripting is also a feature. It should be possible to build scripts from the GUI.

References

[1] Duke, E.M.H., Kehoe, R.C., Rizkallah, P.J., Clarke, J.A. & Nave, C. (1998) Beamline 14: a new multipole wiggler beamline for protein crystallography on the SRS. *J.Synch.Rad.* **5**, 497-499.

[2] Bowler, M., West, J.B., Quinn, F.M., Holland, D.M.P., Fell, B., Hatherly, P.A., Humphrey, I., Flavell, W.R. & Hamilton, B. (2002) A new XUV beamline on a multi-pole wiggler in the *SRS. Surface Review and Letters* **9(1)**, 577-581 .

[3] Bilsborrow, R.L., Dobson, B.R., Cheung, K.C., Dent, A.J., Murphy, L.M., Stephenson, P.C., Hindley, P., Atkinson, P., Bliss, N. & Fell, B. The Daresbury design Sagittal Monochromator, In preparation.

[4] Helsby, W.I., Berry, A., Buksh, P.A., Hall, C.J. & Lewis, R.A. The RAPID2 interpolating system. Presented at SAMBA

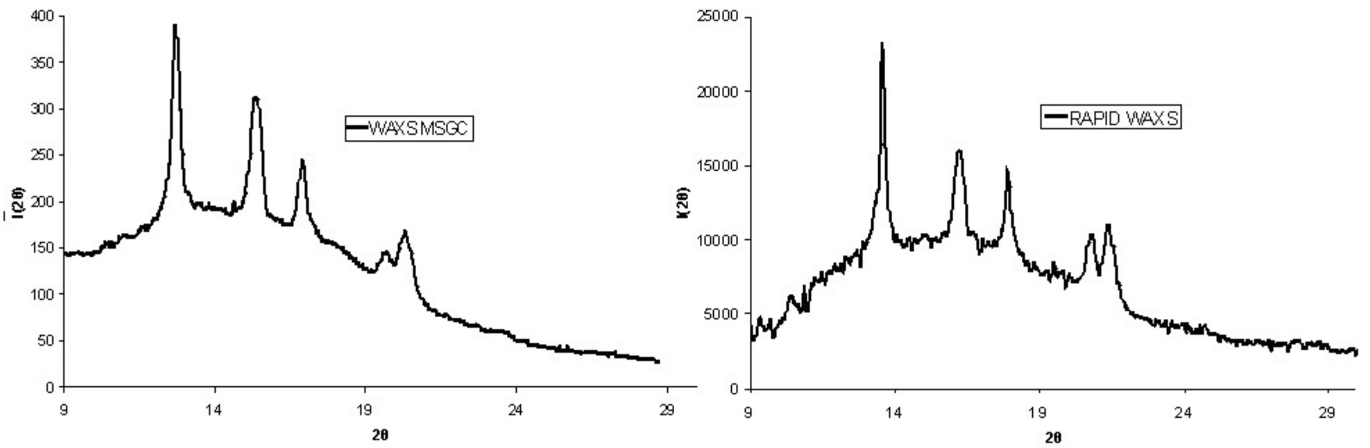

Figure 11: The figure shows a comparison of the same polymer sample collected on the DUBBLE beamline at ESRF (left) and on MPW6.2 (right). It can be seen that the Daresbury data have a higher count rate and better angular resolution but are, at present, slightly noisier.

2, Trieste May 2002, and Submitted to *NIMS-A as conference proceeding*, in press.
[5] Borsboom, M., Bras, W., Cerjak, I., Detollenaere, D., van Loon, D.G., Goedtkindt, P., Konijnenburg, M., Lassing, P., Levine, Y.K., Munneke, B., Oversluizen, M., van Tol, R. & Vlieg, E. (1998) The Dutch-Belgian beamline at the *ESRF. J.Synch.Rad.* **5**, 518-520

Appendix A

1·	**Source Type**	Multipole Wiggler Insertion Device
2·	**Operating Gap**	19.2 mm
3·	**K value**	37.4
4·	**Period**	200 mm
5·	**No of Poles**	9 Full Poles + 2 End Poles
6·	**Peak on axis Field**	2 T
7·	**Peak Flux @ 1.2Å**	4.4 x 1013 (photons/s/mrad/0.1% bw/300mA)
8·	**Critical Wavelength**	2.33 Å @ 0 mR
9·	**Total Power**	2.4 kW @ 300 mA
10·	**Line Power density**	220 W/mrad @ 300 mA
11·	**Peak Power density**	1130 W/mrad2 @ 300 mA